nature geoscience

REVIEW ARTICLE

https://doi.org/10.1038/s41561-018-0146-0

Palaeoclimate constraints on the impact of 2 °C anthropogenic warming and beyond

Hubertus Fischer[1,2*], Katrin J. Meissner[3*], Alan C. Mix[4*], Nerilie J. Abram[5], Jacqueline Austermann[6], Victor Brovkin[7], Emilie Capron[8,9], Daniele Colombaroli[2,10,11,12], Anne-Laure Daniau[13], Kelsey A. Dyez[14], Thomas Felis[15], Sarah A. Finkelstein[16], Samuel L. Jaccard[2,17], Erin L. McClymont[18], Alessio Rovere[15,19], Johannes Sutter[20], Eric W. Wolff[21], Stéphane Affolter[1,2,22], Pepijn Bakker[15], Juan Antonio Ballesteros-Cánovas[23], Carlo Barbante[24,25], Thibaut Caley[13], Anders E. Carlson[4], Olga Churakova (Sidorova)[23,26], Giuseppe Cortese[27], Brian F. Cumming[28], Basil A. S. Davis[29], Anne de Vernal[30], Julien Emile-Geay[31], Sherilyn C. Fritz[32], Paul Gierz[20], Julia Gottschalk[2,17], Max D. Holloway[9], Fortunat Joos[1,2], Michal Kucera[15], Marie-France Loutre[33], Daniel J. Lunt[34], Katarzyna Marcisz[2,11,35], Jennifer R. Marlon[36], Philippe Martinez[13], Valerie Masson-Delmotte[37], Christoph Nehrbass-Ahles[1,2], Bette L. Otto-Bliesner[38], Christoph C. Raible[1,2], Bjørg Risebrobakken[39], María F. Sánchez Goñi[13,40], Jennifer Saleem Arrigo[41], Michael Sarnthein[42], Jesper Sjolte[43], Thomas F. Stocker[1,2], Patricio A. Velasquez Alvárez[1,2], Willy Tinner[2,11], Paul J. Valdes[34], Hendrik Vogel[2,17], Heinz Wanner[2], Qing Yan[44], Zicheng Yu[45,46], Martin Ziegler[47,48] and Liping Zhou[49]

Over the past 3.5 million years, there have been several intervals when climate conditions were warmer than during the pre-industrial Holocene. Although past intervals of warming were forced differently than future anthropogenic change, such periods can provide insights into potential future climate impacts and ecosystem feedbacks, especially over centennial-to-millennial timescales that are often not covered by climate model simulations. Our observation-based synthesis of the understanding of past intervals with temperatures within the range of projected future warming suggests that there is a low risk of runaway greenhouse gas feedbacks for global warming of no more than 2 °C. However, substantial regional environmental impacts can occur. A global average warming of 1–2 °C with strong polar amplification has, in the past, been accompanied by significant shifts in climate zones and the spatial distribution of land and ocean ecosystems. Sustained warming at this level has also led to substantial reductions of the Greenland and Antarctic ice sheets, with sea-level increases of at least several metres on millennial timescales. Comparison of palaeo observations with climate model results suggests that, due to the lack of certain feedback processes, model-based climate projections may underestimate long-term warming in response to future radiative forcing by as much as a factor of two, and thus may also underestimate centennial-to-millennial-scale sea-level rise.

Depending on the choice of future carbon emission scenarios, projected global surface air temperature changes for the end of this century relative to pre-industrial conditions (defined here as average conditions from AD 1850–1900 (ref. [1])) range from 1.6 °C (0.9 to 2.4 °C, 5–95% confidence interval, Representative Concentration Pathway (RCP) 2.6) to 4.3 °C (3.2 to 5.5 °C, 5–95% confidence interval, RCP8.5 (ref. [2])). Models project substantially higher warming at high latitudes, with Arctic temperature changes being amplified in simulations by a factor of 2 to 3, implying future warming of ~3 °C (RCP2.6) to ~12 °C (RCP8.5) in these regions. Moreover, in most areas, the warming is projected to be greater over land than over the ocean.

Even if future emissions are reduced, warming will continue beyond 2100 for centuries or even millennia because of the long-term feedbacks related to ice loss and the carbon cycle[3,4]. Given concern about these impacts, the Paris Agreement proposes reducing emissions to limit global average warming to below 2 °C and pursue efforts to limit it to 1.5 °C, effectively defining a climate 'defence line'[5]. Although this guardrail concept is useful, it is appropriate to ask whether the global limits proposed in the Paris COP21 climate agreement really constitute a safe operating space for humanity[6] on our complex planet.

Many state-of-the-art climate models may underestimate both the rates and extents of changes observed in palaeo data[7]. Models are calibrated based on recent observations, simplifying some processes (for example, the representation of clouds and aerosols) or neglecting processes that are important on long timescales under significantly warmer boundary conditions (for example, ice-sheet dynamics or carbon-cycle feedbacks). This lack of potentially important feedback mechanisms in climate models underscores the importance of exploring warm climate intervals in Earth's history. Understanding these past intervals may illuminate feedback mechanisms that set long-term climate and Earth system sensitivity (ESS), enabling an assessment of the possible impacts of warming on physical, biological, chemical and ecosystem services on which humanity depends.

A full list of authors and affiliations appears at the end of the paper.

Examples of such warmer conditions with essentially modern geographies can be found in Fig. 1 during the Holocene thermal maximum (HTM) and the Last Interglacial (LIG; ~129–116 thousand years ago (ka), where present is defined as 1950). Here, the HTM is broadly defined as a period of generally warmer conditions in the time range 11–5 ka, which, however, were not synchronous in their spatio-temporal expression. The LIG can also be compared to the warmer peak interglacial Marine Isotope Stage (MIS) 11.3 (~410–400 ka), where climate reconstructions exist. Note that these times of peak warmth were associated with different orbital parameters, and thus different spatial and seasonal distribution of solar insolation, while their greenhouse concentrations were close to pre-industrial levels and their temperatures, although within the projected range of anthropogenic warming for the near future, have been controlled by a different blend of forcing mechanisms (see section 'Earth system responses during warm intervals'). Accordingly, past interglacials can be thought of as a series of natural experiments characterized by different combinations of climate boundary conditions[8]. Although they are not strict analogues for future warming, these past warm intervals do illustrate the regional climate and environmental response that may be triggered in the future, and thus remain useful as an observational constraint on projections of future impacts.

The HTM is amenable to detailed reconstruction based on data availability and more refined approaches to chronology, but the older interglacial intervals illustrate greater warming and impacts. To examine past climates with greenhouse gas concentrations of >450 ppm (as expected for RCP2.6), we must look farther back in time, to the mid-Pliocene warm period (MPWP), 3.3–3.0 million years ago (Ma), when atmospheric CO_2 was between 300 and 450 ppm[9] (Fig. 1) and warm conditions lasted long enough to approach equilibrium. Older intervals, such as the early Eocene climatic optimum (EECO, ~53–51 Ma) offer an opportunity to study extremely high-CO_2 scenarios (900–1,900 ppm) that are comparable with the fossil-fuel-intensive RCP8.5 scenario[2,10] (>1,200 ppm); however, these older intervals had continental configurations significantly different from today.

Palaeo evidence over the last 2,000 years and during the Last Glacial Maximum (LGM) was discussed in detail in the Fifth Assessment Report of the Intergovernmental Panel for Climate Change[2]. Here, we focus on the climate system responses during the three best-documented warm intervals, the HTM, LIG and MPWP (Figs. 1 and 2), and address spatial patterns of environmental changes and the forcing leading to them. Observations on the spatial temperature expression of these warm periods and their forcing are presented in Box 1, which also includes a discussion of the limitations of these time intervals as first-order analogues for future global and regional warming. Palaeo evidence on the Earth system response to these warmer conditions is reviewed in the next section (summarized in Fig. 3). The section 'Amplification and thresholds: palaeo lessons for the future' discusses potential feedbacks and thresholds in the climate system in light of the palaeo record and their implications for future warming impacts. Based on the palaeo evidence on climate, sea level and past CO_2 in warm intervals, we assess the long-term ESS[11] as imprinted in the palaeo record in Box 2 and draw conclusions on limitations of current climate models to predict the long-term (millennial) change in Earth's climate. Given its different continental configuration, we limit our analysis of the EECO to the issue of ESS in Box 2, based on available palaeo data and published model experiments where we account for the global effects of changing distribution of landmasses at that time.

Earth system responses during warm intervals

Changes in temperature conditions lead to significant regional responses in the Earth system. In the following sections, past changes in important components of the Earth system are summarized, for which the palaeo record allows us to draw conclusions for a future warming of 2 °C and beyond.

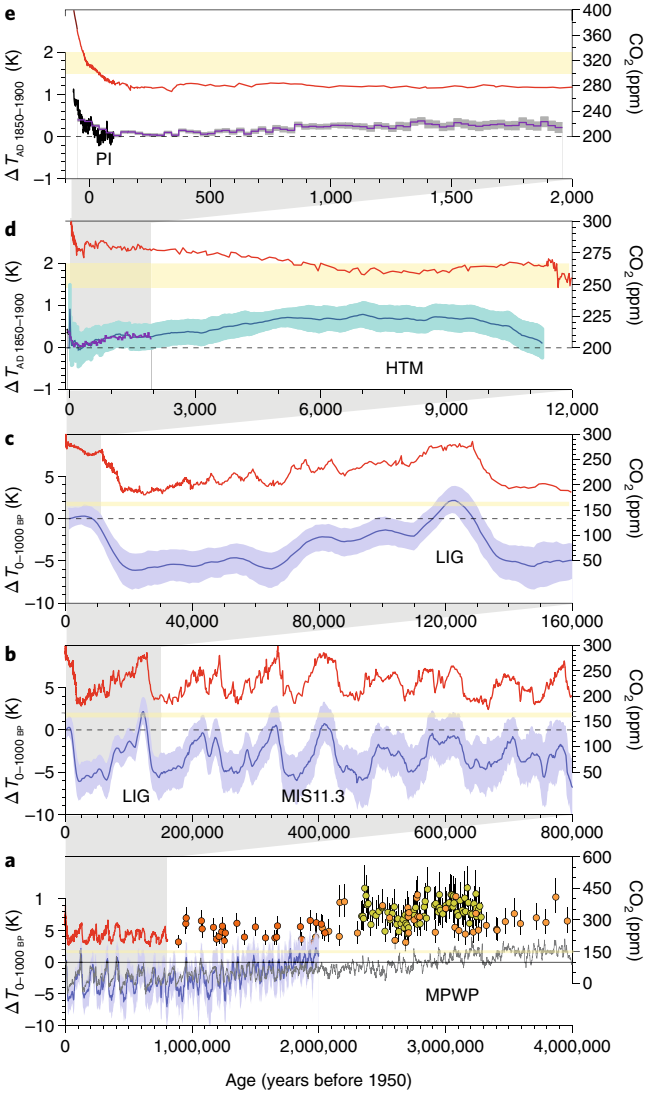

Fig. 1 | Changes in global climate and radiative forcing over the last 4 Myr. **a**, Changes in global surface air temperature (GSAT: Snyder[103] (blue line) with 2.5% and 97.5% confidence intervals (light blue shading), Hansen et al.[104] (grey line)) reconstructed from proxy records (left *y*-axis) and changes in atmospheric CO_2 (right *y*-axis) from ice-core air bubbles (red line: Bereiter et al.[69]) and marine CO_2 proxies (light orange dots: Bartoli et al.[105]; dark orange dots: Hönisch et al.[106]; green dots: Martinez-Boti et al.[9]) over the last 4 Myr. **b**, Same as in **a** for the last 800,000 years. **c**, Same as in **a** and **b** for the last 160,000 years. **d**, GSAT reconstructed from proxy records by Marcott et al.[107] over the Holocene (blue line with 2.5% and 97.5% uncertainty limits in light blue shading) and the Past Global Changes (PAGES) 2k Consortium[108] (purple line) together with changes in atmospheric CO_2 from ice-core air bubbles (red line[69]). **e**, Measured GSAT over the last 150 years (HADCRUT4 (ref. [1], black line)) and reconstructed from proxy records over the last 2,000 years[108] (purple line, 30 bins with 2.5% and 97.5% bootstrap confidence limits in grey shading) together with changes in atmospheric CO_2 from ice-core air bubbles (red line[69]) and globally averaged atmospheric observations (data from https://www.esrl.noaa.gov/gmd/). Note that temperatures in **d**–**e** are given as anomalies relative to the pre-industrial mean, where pre-industrial is defined as the time interval 1850–1900. Proxy data in **a**–**c** are not available in sufficiently high resolution to unambiguously quantify a mean for this short time interval. Accordingly, panels **a**–**c** are given relative to an extended pre-industrial reference time interval of the last 1,000 years. The horizontal yellow bars indicate the 1.5–2 °C warming target relative to pre-industrial of the Paris agreement. *T*, temperature; PI, pre-industrial.

Box 1 | Global and regional temperature changes in past warm intervals

The HTM surface warming relative to pre-industrial conditions was on average <1 °C (ref. [107]) and is mostly expressed in Northern Hemisphere proxies that are sensitive to the warm season. Although some regional studies define the HTM narrowly as older than 8.2 ka, here we take a broad definition of ~11–5 ka. We exclude the 8.2 ka cold event in the North Atlantic region, which is thought to have been caused by a freshwater disturbance[111] in the North Atlantic and subsequent weakening of the AMOC, and is not representative of a global warming response expected for the end of this century.

The HTM was a complex series of events in which warming occurred while ice cover and sea level had not reached postglacial equilibrium and continental ice sheets in North America and Scandinavia were still retreating. This complexity of residual ice cover makes it likely that HTM warming was regional, rather than global, and its peak warmth thus had different timing in different locations[10]. Ice-core data show that radiative forcing due to greenhouse gases during the HTM was slightly lower than pre-industrial values[112]. Compared to pre-industrial conditions, the HTM orbital configuration featured greatly enhanced summer insolation in high northern latitudes and reduced winter insolation below the Arctic Circle. On an annual average, HTM insolation was higher at high latitudes, but slightly lower in the tropics[113].

Global-average and high-northern-latitude surface temperatures during the HTM appeared to be warmer (at least during summer) than today, while low-latitude climates were slightly cooler[107], consistent with annual orbital forcing. Although substantial warming was found in the North Atlantic marine sector between 11 and 5 ka (ref. [107]), recent reconstructions of climate in the mid-northern latitudes of continental North America and Europe based on pollen data were characterized by a cooler HTM with a slow warming as the continental ice sheets retreated[114]. In contrast, Greenland's mean annual atmospheric temperature (after correction for ice-sheet altitude changes) peaked earlier, between 10 and 6 ka (refs [115,116]), and was warmer than pre-industrial by 1–4 °C (ref. [117]), while the Nordic seas were only warmer by ~0.5–1 °C (ref. [118]). The North Pacific Ocean also displayed an early Holocene warming, and in most areas a mid-Holocene cooling relative to today, but warming in the North Pacific and East Asia occurred earlier than in the Atlantic sector. Peak warming in the Bering Sea (1–2 °C), the western subpolar North Pacific (1–2 °C) and the Sea of Okhotsk (2–3 °C) occurred between 9 and 11 ka, with a possible second warm event between 7 and 5 ka in the Sea of Okhotsk[119]. In the subpolar Northeast Pacific off Alaska, peak warming (~1 °C above modern, ~3–4 °C above mid-Holocene) occurred near 11 ka (ref. [33]), and in the Pacific off Northern California, peak warmth occurred in two events near 11 ka and again near 10 ka (ref. [120]).

In summary, the HTM is a complex regional series of events, best expressed at higher northern latitudes, earliest in the North Pacific marine sector, substantially delayed on land areas influenced by residual ice, and slightly delayed in the North Atlantic and Greenland sector relative to North Pacific and East Asian locations. Although its regional expression makes it difficult to draw a unique global picture, it nevertheless serves as a well-dated and data-rich example of regionally warmer conditions, and is instructive for the impact of warming in these environments. Its complexity also suggests caution in over-interpreting older intervals as being representative of global climate states, because less data are available and chronological constraints are weaker.

The LIG global-average sea surface temperature (SST) was probably 0.5–1 °C warmer than pre-industrial at least seasonally[109,121–123] (Supplementary Table 2). Here, we use the value of 0.5 ± 0.3 °C as best estimate of the global SST warming at 125 ka (ref. [109]), a time period when also the northern hemisphere reached a stable warm plateau, although global SST peak warmth may have been somewhat earlier[123]. Using a general scaling of global SST to global surface temperature[103] of 1.6, this implies that global surface temperature was probably ~0.8 °C (maximum 1.3 °C) warmer than pre-industrial[124] and followed a strong orbitally induced maximum in Northern Hemisphere summer insolation after a rise in atmospheric CO_2 concentrations from low ice-age values to levels only slightly higher than pre-industrial (latest data compiled by ref. [69]). Similar to the HTM, significant spatial and temporal differences in the expression of the warming exist; extratropical regions showed more pronounced warming, while tropical regions showed only little warming[124] or even a slight cooling[109] in line with modelling results[110]. Temperature reconstructions show a pronounced polar amplification signal in the Arctic during the LIG (see Fig. 2), with northern high-latitude oceans warming by >1–4 °C and surface air temperatures by >3–11 °C (refs [46,125,126]) relative to pre-industrial. As with the HTM, the LIG warming caused by higher northern summer insolation appears to be more representative for regional high-latitude warming than for low-latitude warming in the future.

The MPWP was subject to intermittently elevated CO_2 (potentially up to 450 ppm) compared to the HTM and the LIG[9]. The CO_2 concentration at that time was most similar to the RCP2.6 scenario, and a factor of three-to-four less than concentrations expected by AD 2100 for the RCP8.5 scenario. Climate models simulate an increase in tropical temperatures by 1.0–3.1 °C (for RCP2.6 CO_2 forcing of 405 ppmv (ref. [2])), generally in line with MPWP proxy reconstructions at low latitudes[127]. Strong polar amplification is observed for the MPWP. For example, proxy data from the North Atlantic and northeastern Russian Arctic indicate a rise of surface air temperatures by 8 °C (ref. [128]) during the MPWP and even higher in the early Pliocene[129]. These regional temperature changes are similar to projected warming at AD 2100 for the RCP8.5 scenario, in spite of the much lower CO_2 rise during the MPWP, and suggest that current models may underestimate the warming response in the Arctic[130] to increased CO_2 concentrations.

Continental ice sheets and changes in sea level. Although alpine glaciers, parts of the Greenland Ice Sheet (GIS) and some sectors of Antarctica may have had less ice during the HTM than today[12,13], sea level was still ~26 m (9 ka) to ~2 m (5 ka) lower than present[14], implying the presence (but ongoing melting) of remnants of the glacial maximum continental ice sheets. Greenland ice retracted to its minimum extent between 5 and 3 ka, perhaps as a slow response to HTM warming[15].

Global sea-level reconstructions of 6–9 m higher than present during the LIG (and at least that for MIS11.3) require a substantial retreat of at least one of the Greenland and Antarctic ice sheets, but probably a significant reduction of both, relative to their current volumes[16]. During the LIG, the marine-terminating ice sheet in southern and central Greenland retreated to terrestrial margins[17]. While latest ice-sheet and climate model simulations allow for a substantial retreat of the West Antarctic Ice Sheet (WAIS) and potentially parts of East Antarctica[18,19], direct observational evidence is still lacking. The GIS was also significantly reduced during MIS11.3 peak warming with only a remnant ice cap in the northern part of Greenland[20]. Cosmogenic exposure dating of subglacial materials under Summit, Greenland, suggest loss of part of the GIS during some warm intervals of the Pleistocene[21].

Ice sheets existed in Greenland and Antarctica during the MPWP, but their configuration is uncertain[18,22]. A reconstructed sea-level

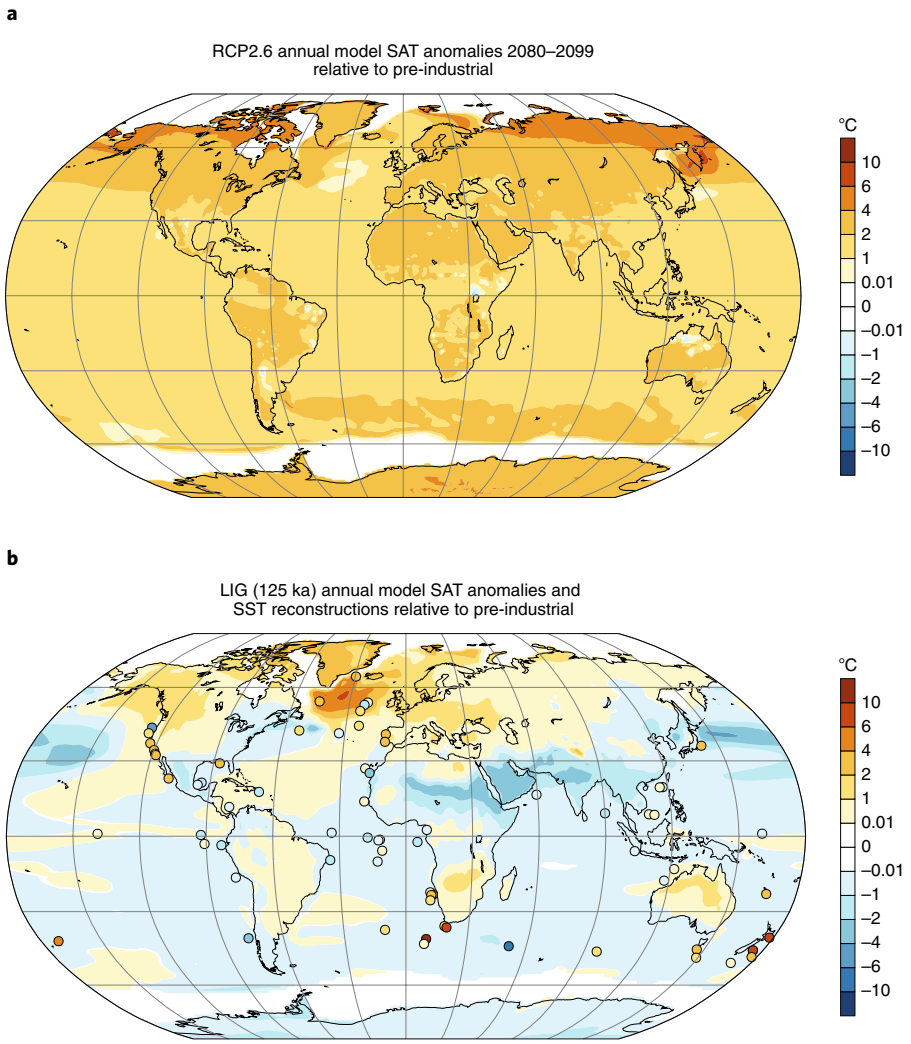

Fig. 2 | Model–data comparison of climate changes in the future and during the LIG. a, RCP2.6 model ensemble (CCSM4) results of mean annual surface air temperature (SAT) anomalies for the time interval 2080–2099 relative to our pre-industrial reference interval, 1850–1900. **b**, Observed LIG (125 ka) annual sea surface temperature (SST) anomalies[109] relative to its reference period of 1870–1889 (dots) overlain on top of CCSM3 SAT anomalies for the 125 ka time window relative to 1850 (ref. [110]). White areas in polar regions in panels **a** and **b** represent the modelled sea ice extent.

rise of 6 m or more implies substantially less global ice than present (upper limit poorly constrained) during the MPWP[16], and this calls for a significant shrinkage of the GIS and/or AIS. Model results suggest a significantly reduced GIS[23], while geological data show evidence of West Antarctic deglaciation[24] and potentially also over the Wilkes subglacial basin in East Antarctica[25].

Sea ice. Qualitative reconstructions of sea ice extent and concentrations suggest reduced extent during past warm intervals both in the Arctic and around Antarctica[26,27]. However, even during the LIG, with strongly elevated summer insolation, sea ice existed in the central Arctic Ocean during summer, whereas sea ice was significantly reduced along the Barents Sea continental margin and potentially other shelf seas[28]. Ice-core evidence for the LIG has been interpreted as suggesting that multi-year sea ice around Greenland was reduced, but winter sea ice cover was not greatly changed[29]. In the Southern Ocean, reconciliation of climate model output with warming evidence from Antarctic ice cores suggests that Antarctic winter sea ice was reduced by >50% at the onset of the LIG[30]. However, although this reconstruction is consistent with a compilation of Southern Ocean sea ice proxy data, most published marine core sites are situated too far north for independent verification[30].

Based on limited observational evidence, generally reduced summer sea ice cover in the Arctic Basin has been reconstructed during the MPWP[23] and biomarkers at the Iceland Plateau indicate seasonal sea ice cover with occasional ice-free intervals. During this warm interval, the East Greenland Current may have transported sea ice into the Iceland Sea and/or brought cooler and fresher waters favouring local sea ice formation[31].

Marine plankton ecosystem changes. Warmer ocean temperatures influenced marine ecosystems. The HTM warming was regionally diachronous and therefore did not leave a globally consistent fingerprint on the surface-layer plankton habitat[32]. There is nevertheless abundant evidence for changes in productivity, such as in the North Pacific, where early Holocene warming appears to have promoted diatom blooms and enhanced export production in warmer, more-stratified surface waters[33].

A reorganization of ocean productivity was also documented during the LIG, with evidence for increased frequency and poleward expansion of coccolithophore blooms[34] and higher export production in the Antarctic Zone of the Southern Ocean[35,36]. Strongly increased export production is also found in the Southern Ocean during the MPWP[37]. The impacts of these changes on higher

trophic levels and benthic ecosystems remain unexplored, except in the climatically sensitive marginal seas. Here, circulation changes during past warm intervals led to local extinctions and community reorganization in marine ecosystems[38], with a stronger response to LIG climate forcing than in the Holocene.

Whereas HTM and LIG marine communities are good compositional and taxonomic analogues to the present, MPWP marine ecosystems differ due to substantial species turnover (extinctions and originations)[39]. In some groups of plankton, such as in planktonic foraminifera, enough extant species existed in the MPWP to judge general ecosystem shifts[40]. Data from these groups indicate that poleward displacement of mid- and high-latitude marine plankton during the MPWP was stronger than during the LIG, but the diversity–temperature relationship remained similar and comparable to the present[41]. Thus, oceanic marine plankton responded to warming with range shifts, rather than by disruption of community structure.

Vegetation and climate on land. Extensive proxy data is available from all continents showing large changes in vegetation and shifts in moisture regimes, indicating that the HTM was complex and temporally variable. For example, major HTM changes in vegetation are marked by greening of the Sahara[42], whereas in other regions, including the Northern Great Plains of North America, aridity increased and expanded east into the boreal biome[43]. Many regions experienced a climate-driven poleward extension of their biome boundaries with similar altitudinal vegetation expansions by a few hundred metres[44]. The tundra and tundra–forest boundary in eastern North America, Fennoscandia and Central Siberia shifted northward (by ~200 km), while forest shifted southward in eastern Canada (by ~200 km)[45].

During the LIG, tundra vegetation[46] contracted, the Sahara Desert vanished[47], and boreal forest vegetation[48] and savanna[47] expanded. Temperate taxa (hazelnut, oak, elm) were found north of their current distribution in southern Finland[49]. In Siberia, birch and alder shrubs dominated vegetation compared to herb-dominated tundra at present[50]. Southwestern Africa was marked by expansion of Nama Karoo and fine-leaved savanna[51].

In the MPWP, temperate and boreal vegetation zones shifted poleward (for example in East Asia and Scandinavia[52]). Tropical savannas and forests expanded, while deserts contracted[23].

Amplification and thresholds: palaeo lessons for the future

Understanding potential amplification effects and non-linear responses in climate and environmental systems is essential, as they have substantial environmental and economic consequences[53]. Many potential amplification effects are outside of historical human experience, so palaeo data may help understand these processes.

Carbon-cycle feedbacks. Radiative forcing over the last 800,000 years by the atmospheric greenhouse gases CO_2, CH_4 and N_2O was often lower but rarely higher than pre-industrial values[54], and greenhouse gas rise rates in past warm periods were much slower. Over the period 1987–2016, global annual greenhouse gas concentrations rose on average by 19 ppm per decade for CO_2 (with generally increasing rise rates over this 30 year interval), by 57 ppb per decade for CH_4 and by 8 ppb per decade for N_2O (all data from https://www.esrl.noaa.gov/gmd/), while during the last deglaciation, high-resolution ice-core data (WAIS Divide and Taylor Glacier, Antarctica) reveal natural rise rates up to a factor of 10 slower (~2 ppm per decade for CO_2, ~20 ppb per decade for CH_4, and ~1 ppb per decade for N_2O (refs [54–56])). While these natural variations in greenhouse gas forcing represent a substantial contribution to glacial–interglacial climate variations, the climate mechanisms that drive changes in the carbon cycle and the associated climate feedbacks remain a matter of debate.

Analyses of last millennium CO_2 and northern hemisphere temperature variability suggest a warming-driven net CO_2 release from the land biosphere (2–20 ppm per °C) on decadal-to-centennial scales[57,58]. During short-term warming events in pre-industrial times (when CO_2 was rather constant), net release of land carbon due to enhanced respiration of soil and biomass appears to compensate plant growth associated with fertilization effects by higher temperatures. A similar short-term response can be expected for future regional warming.

Peat accumulation rate is positively correlated with summer temperature[59], but is a relatively slow process. Peat reservoirs have gradually increased over the Holocene, resulting in long-term sequestration of carbon[60]. HTM rates for net carbon uptake by northern peatlands were clearly higher than those for the cooler late Holocene[61,62] as a result of rapid peatland inception and peat growth during times of ice-sheet retreat and strong seasonality.

While peatlands were present during the LIG[63], the preserved record is fragmentary so the magnitude of LIG peat carbon storages is not well constrained. During the Pliocene (and MIS11.3), peats were probably abundant but there are only a few dated peat deposits of this age (for instance, German and Polish lignite[64]). Boreal-type forested peatlands with thick peat accumulations may have accumulated over >50,000 years in response to warmer climates during the Pliocene[65].

Based on these palaeo-environmental analogues, peatlands will probably expand in a 2 °C warmer world on centennial-to-millennial timescales, although the size of this sink is difficult to estimate based on the palaeo record alone and the net carbon source or sink may depend on the rate of warming and moisture conditions. If warming is fast (decadal-to-centennial), carbon may be released via respiration faster than it can accumulate via peat growth. If warming is slower (centennial-to-millennial) continued peat growth may outstrip respiratory losses, yielding a net carbon sink.

Widespread permafrost thaw and enhanced fire frequency and/or severity could counteract carbon sink effects of long-term peat growth[66]. Today, about 1,330–1,580 gigatons of carbon (GtC) are stored in perennial frozen ground, of which ~1,000 GtC (more than the modern atmospheric carbon inventory) are located in the upper 0–3 m of soil. This frozen carbon is susceptible to a thawing of the upper permafrost layer under future warming[67] and risks of the related carbon release can be assessed in ice-core gas records. Although detailed data are limited, the observed variation of CO_2 and CH_4 in ice-core records suggests that the risk of a sustained release of permafrost carbon is small if warming can be limited to the modest high-latitude warming encountered during past interglacial periods[68]. Apart from short-lived positive excursions observed at the onset of many interglacials, atmospheric CH_4 and CO_2 concentrations in the ice record[69,70] were not significantly elevated in past interglacials in which the Arctic was significantly warmer than during pre-industrial times[50]. Accordingly, the additional CO_2 and CH_4 releases at the onset of interglacials (if they were related to permafrost warming[71]), were not sufficient or long enough to drive a long-term 'runaway' greenhouse warming that outpaces negative feedback effects. If future warming is much greater than that observed for past interglacials, release of carbon from permafrost remains a serious concern that cannot be assessed based on the palaeo evidence presented here.

A release of CH_4 from marine hydrates during climate warming, as suggested from marine sediment records[72], cannot be confirmed. Isotopic analysis of CH_4 preserved in ice cores suggests that gas hydrates did not contribute substantially to variations in atmospheric CH_4 during rapid warming events in the glacial and deglacial[73,74]. This may suggest that long-term CH_4 releases are also unlikely to occur in future warming, as long as the magnitudes and rates of warming are limited to the range observed in the geologic record of past warm intervals.

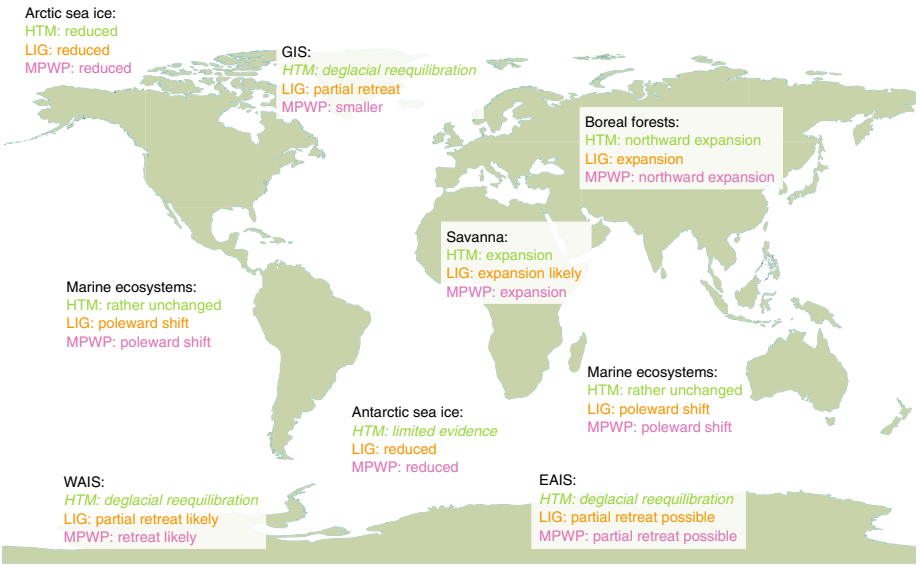

Fig. 3 | Impacts and responses of components of the Earth system. The figure summarizes the statements in the second and third sections ('Earth system responses during warm intervals' and 'Amplification and thresholds: palaeo lessons for the future') in extremely condensed form (all statements relative to pre-industrial). Responses where other reasons prohibit a robust statement are given in italic. Additional evidence that is either not applicable for the future warming or where evidence is not sufficient to draw robust conclusions is summarized in the Supplementary Information. Note that significant spatial variability and uncertainty exist in the assessment of each component and, therefore, this figure should not be referred to without reading the text in detail.

Based on the evidence summarized above, the risk of future massive terrestrial CH_4 or CO_2 releases that may lead to a runaway greenhouse gas effect under modest warming scenarios of RCP2.6 appears to be limited. However, the amount of carbon released from permafrost as CO_2 may amount to up to 100 GtC (ref. [75]) and has to be accounted for when implementing policies for future allowable anthropogenic carbon emissions. We cannot rule out net release of land carbon if future warming is significantly faster or more extensive than observed during past interglacials. Furthermore, past increases in CO_2 were mostly driven by changes in the physical and biological pumps in the ocean and—on long timescales—through interactions between ocean and sediments and the weathering cycle. The reconstruction of ocean carbon reservoirs during past warm episodes remains a challenge, and the risk of significant reductions of ocean CO_2 uptake or disturbances in the Atlantic meridional overturning circulation (AMOC) in the future with feedbacks on the carbon cycle are not well constrained.

Thresholds for ice-sheet melting. Models of the GIS suggest extensive and effectively irreversible deglaciation above a certain temperature threshold, but the threshold is model dependent[76,77]. Marine records of southern GIS sediment discharge and extent suggest that the GIS was substantially smaller than present during three out of the last five interglacials[78] with near-complete deglaciation of southern Greenland occurring during MIS11.3 (refs [20,79]). This suggests that the threshold for southern GIS deglaciation has already been passed for the polar temperature amplification signal associated with a persistent global warming by 2 °C, that is, within the range of the Paris Agreement (see Fig. 2). Concentrations of cosmogenic radionuclides in bedrock at the base of Summit Greenland have been interpreted to suggest multiple periods of exposure of the western GIS during the last million years[21]. In contrast, the age of the basal ice at Summit Greenland suggests a persistent northern Greenland ice dome at least for the last million years[79]. Vice versa, the southern Greenland ice dome existed during the LIG but melted at some time before 400 ka (ref. [79]). Marine records suggest the persistence of ice in eastern Greenland for at least the last 3 million years[80], which would imply different temperature thresholds for deglaciation of different parts of the GIS.

The WAIS was appreciated by AR5 (ref. [2]) and previous assessments as possessing an unstable marine-based geometry, but the thresholds at which strong positive feedbacks would be triggered were unknown, and models failed to reproduce past sea-level contributions[2]. Several lines of observational evidence suggest episodes of major retreat of marine WAIS sectors[81,82]. Marine-based sectors of the East Antarctic Ice Sheet (EAIS) are now known to be at similar risk of collapse as those of the WAIS[25,83]. The main indicator for a substantial AIS contribution to global sea-level rise in past interglacials remains the sea-level proxy record[16]. The survival of parts of the GIS in the LIG requires a significant retreat of at least part of the AIS. Pliocene reconstructions of sea-level highstands require a substantial contribution of both the WAIS and EAIS but are subject to major uncertainties[16].

Since AR5, model simulations are now more consistent with prior theory and sea-level constraints[18,19,84]. Ice-sheet model simulations suggest that marine ice-sheet collapse can be triggered in sectors of the EAIS and WAIS for a local sub-surface ocean warming of +1–4 °C (refs [18,19,84]). However, thresholds for Antarctic marine ice-sheet collapse vary considerably between models and their parameterizations of ice-shelf mass balance and ice dynamics[18,19,84]. While some models predict that Antarctica is now more sensitive than the literature assessed in AR5 (ref. [2]), the current geological record[85,86] and modelling evidence are not sufficient to rule out or confirm tipping points for individual Antarctic sectors within the 1.5–2 °C global warming range.

Of special societal relevance is also the rate of sea-level increase. Sea-level rise has accelerated over the last century from 1.2 ± 0.2 mm yr^{-1} between 1901 and 1990 (largely due to thermosteric effects) to 3.0 ± 0.7 mm yr^{-1} over the last two decades as net melting of glaciers and ice sheets has increased[87]. Records of palaeo sea-level rise rates expand our view into times when the melting response of the GIS and AIS may have been much larger than today. Sea-level changes

Box 2 | Constraining climate sensitivity from past warm periods

Fundamental to projecting future warming and impacts is the climate sensitivity to radiative greenhouse forcing, that is, the global-average surface air temperature equilibrium response to a doubling of CO_2. The multi-model mean equilibrium climate sensitivity of the Coupled Model Intercomparison Project Phase 5 (CMIP5) is 3.2 ± 1.3 °C (ref. [2]). These models include most of the 'fast' feedback processes that result in the 'Charney Sensitivity' (CS), but lack some other important processes. In particular, many models do not include some of the real-world 'slow' feedback processes relevant for the Earth's total warming response, such as long-term changes in ice sheets, sea level, vegetation or biogeochemical feedbacks that may amplify or reduce the amount of non-CO_2 greenhouse gases in the atmosphere. Furthermore, our understanding of some atmospheric processes under warmer boundary conditions, such as those associated with cloud physics and aerosols, is still limited. The climate models therefore cannot be expected to include realistic long-term feedbacks, which leads to increased uncertainty in climate sensitivity. The long-term climate sensitivity including all these processes is called the Earth system sensitivity (ESS).

Direct correlation of Pleistocene CO_2 and temperature reconstructions suggest ESS values of 3–5.6 °C (refs [131,132]). These estimates are based on climate change during glacial cycles. They are therefore indicative of sensitivities associated with large varying glacial ice sheets, and may, therefore, not be appropriate for future warming[11,133]. When corrected for land-ice–albedo feedbacks, vegetation and aerosols, climate sensitivities implied by these geological estimates may have been 30–40% lower[134].

We revisit this issue, comparing our palaeoclimate data synthesis from episodes warmer than today, with published long transient model simulations 10,000 years into the future[3] based on a range of CO_2 emission scenarios with two fully coupled climate–carbon-cycle Earth system models of intermediate complexity (UVic and Bern3D-LPX)[3]. Both models include fully coupled ocean, atmosphere, sea ice, dynamic vegetation and ocean-sediment models with offline ice-sheet models[3]. Furthermore, we include a published series of equilibrium climate simulations with four dynamic atmosphere–ocean general circulation models, with primitive equation atmospheres (HadCM3L, CCSM3, ECHAM5/MPI-OM, GISS ModelE-R) and one model of intermediate complexity (UVic) under early Eocene boundary conditions[10,135].

In the figure below, we compare global surface air temperature anomalies (relative to pre-industrial) to CO_2 (panel a), ESL rise relative to CO_2 (panel b), and sea-level rise relative to surface air temperature anomalies (panel c). Palaeo data represent the three episodes (HTM, LIG, MPWP) discussed earlier; however, HTM sea-level data are excluded as sea level is still strongly increasing by deglacial ice-sheet melt at that time. To expand the range of climate boundary conditions, we also include data from the EECO (~53–51 Ma), when CO_2 was around 1,400 ppm and within a likely range of ~900 to 1,900 ppm (ref. [136]). EECO conditions include changes in the configuration of the continents, land surface topography

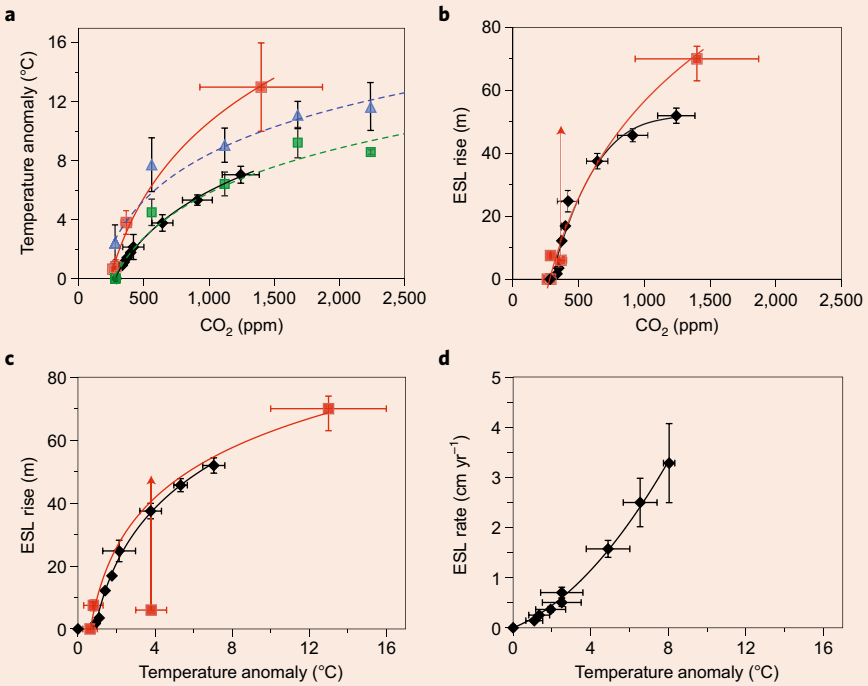

Temperature and sea-level response to CO_2 forcing. a, Annual and global mean surface air temperature anomalies (relative to pre-industrial) as a function of atmospheric CO_2 concentrations (see Supplementary Tables 1 and 2). **b**, ESL rise relative to CO_2 levels (see Supplementary Tables 8 and 10). **c**, ESL rise relative to surface air temperature anomalies. **d**, Peak rates of ESL rise as a function of coeval surface air temperature anomalies. Black diamonds show simulations of future scenarios by two models of intermediate complexity[3], blue triangles are model ensemble mean equilibrium simulations under EECO boundary conditions[10,135], green squares show EECO simulation responses due to changes in CO_2 concentrations alone, estimated by removing the effects associated with the planetary surface boundary conditions relative to pre-industrial control, and red squares are palaeoreconstructions (Supplementary Tables 8–11). Atmospheric CO_2, surface air temperatures and ESL-level values are averaged over AD 10000–12000 in future simulations (black diamonds, **a**–**c**). Peak rates of simulated sea-level rise occur earlier, between the twenty-third and twenty-sixth centuries AD, and are compared to coeval transient model temperatures. The red arrows in **b** and **c** indicate minimum uncertainties. For ESLs (**b**–**d**), EECO values include melting of the full modern inventory of ice, plus steric effects (see Supplementary Table 10 for details). Changes in ocean basin shape are excluded from the EECO ESL calculation.

Box 2 | Constraining climate sensitivity from past warm periods (Continued)

and albedo changes for loss of continental ice sheets. To separate fast and slow feedbacks, we show EECO model ensemble surface air temperature anomalies, including all boundary conditions (blue triangles) and values extracting the component related to modified land surface albedo due to the removal of ice sheets (green squares), in panel a of the figure. Model simulations suggest that the loss of ice at the EECO accounts for 0.2 to 1.2 °C (ref. [137]).

Transient model projections of future warming in response to CO_2 (panel a, black diamonds; see Supplementary Tables) indicate model ESS of ~3 °C, a factor of two lower than inferred from the palaeo data for the EECO (red squares, see also Supplementary Tables 1 and 2). EECO model ensemble estimates of warming (after removing the effect of changing surface albedo, green squares) are essentially identical to the transient future runs. The EECO simulations that include the effect of surface albedo (blue triangles) are closer to the palaeo reconstructions, but still underestimate the inferred EECO warming at high CO_2, so including interactive land ice as a feedback is essential to reproduce the ESS derived from palaeo evidence. This finding echoes previous concern that models built to reproduce present-day climate conditions may be insufficiently sensitive to long-term change[7].

For modest CO_2 rises associated with the MPWP, modelled sea-level changes are generally consistent with palaeo data, but for larger CO_2 rises the models underestimate the largest sea-level rise, such as those reconstructed with larger uncertainties for the EECO (panel b). The UVic model appears to have reasonable sensitivity for the relationship between sea-level rise and warming (panel c; note uncertainty of the ESL rise for MPWP). The underestimation of observed past sea-level rises by the models is therefore probably due to an underestimation of warming. This misfit becomes important because the rate of sea-level rise in the models is dependent on the extent of warming (panel d). If the models were more sensitive to radiative forcing in particular on long timescales (by up to a factor of two, if they are supposed to fit the palaeoclimate data), this would imply an increase by a factor of two to three in the rate of sea-level rise.

While simulations of climates similar to present-day conditions, such as the HTM, agree reasonably well with palaeo records, the differences become more substantial for climates that were significantly warmer (MPWP, EECO), but which are also subject to larger uncertainties in temperature and CO_2 reconstructions. Climate models underestimate polar amplification (see section 'Continental ice sheets and changes in sea level') in the Arctic, as well as global mean temperatures, and therefore also underestimate the extent and rate of sea-level rise. Hence, climate models are still missing or misrepresenting key processes needed to simulate the dynamics of warmer climates on long timescales. Potential caveats include misrepresentations of cloud physics and aerosols[138,139], ocean and atmosphere circulation changes, and insufficient representations of ice-sheet and carbon-cycle feedbacks.

Although state-of-the-art climate models plausibly have correct sensitivity for small magnitude and near-term projections (such as RCP2.6 at year 2100), they can be questioned to provide reliable projections for large magnitude changes (such as RCP8.5) or long-term climate change (beyond 2100), when Earth system feedbacks become important, and for which the models probably underestimate sensitivity.

within the LIG were likely between 3 and 7 mm yr^{-1} (1,000-year average), with a 5% probability of >11 mm yr^{-1} (ref. [88]). For example, exposed fossil coral reefs from Western Australia[89] suggest that, after a period of eustatic sea level (ESL) stability (127 to 120 ka), sea level rose quite quickly from 2.5 to nearly 8.5 metres in less than 1 kyr (that is, 6 mm yr^{-1}). Indirect evidence for sea-level rise from Red Sea isotopic measurements within the LIG allows rise rates as high as 16 mm yr^{-1} (ref. [90]). All of these estimates are uncertain for both level and chronology and are subject to regional isostatic effects but multimetre-scale sea-level oscillations within the last interglacial cannot be excluded[16]. They highlight the possibility that future sea-level rise may be significantly faster than historical experience as also suggested in recent satellite altimeter data[91].

Response of land ecosystems. The palaeo record suggests sensitivity of forest ecosystems, specifically in ecotone positions, to moderate warming (1–2 °C) at the decadal-to-centennial scale[92,93], with tipping points reached in regions where moisture availability will go below critical ecophysiology levels for trees[94]. At higher latitudes and in mountain ranges, increased temperatures will promote forest expansion into tundra[95]. Such northward shifts of boreal ecosystems will be counterbalanced by forest die-back in areas where increased drought will instead favour open woodlands or steppe[96].

Evidence from the HTM suggests that cool-temperate and warm-temperate (or subtropical) forests may collapse in response to climate warming of 1–2 °C, if moisture thresholds are reached[97], and flammable, drought-adapted vegetation will rapidly replace late-successional evergreen vegetation in Mediterranean areas[98].

Substantial and irreversible changes are also expected for tropical forests, with large-tree mortality occurring where peripheral areas of rainforest will turn into self-stabilizing, fire-dominated savanna[99]. The Green-Sahara–desert transition that occurred at the end of the African Humid Period[100] implies that a warmer climate may cross the threshold to open, fire-maintained savanna and grassland ecosystems. Such rainfall thresholds are more easily reached with deforestation, and imply increased flammability, reduced tree reestablishment, and rapid runaway change toward treeless landscapes[99]. Opposed to carbon reduction in tropical forests is fuel build-up in subtropical regions under increasing-rainfall scenarios[2], implying that critical transitions will be spatially complex, depending on the position along moisture gradients[96,99].

Conclusions

Past warmer worlds were caused by different forcings, which limits the applicability of our findings to future climate change. Nevertheless, we can conclude that even for a 2 °C (and potentially 1.5 °C) global warming—as targeted in the Paris Agreement[101]—significant impacts on the Earth system are to be expected. Terrestrial and aquatic ecosystems will spatially reorganize to adapt to warmer conditions as they did in the past (for example, during the HTM or LIG). However, human interferences other than climate change, such as pollution, land-use, hunting/fishing and overconsumption, appear to have a much larger influence on species extinction and diversity loss[102] than climate warming.

The risk of amplification, such as runaway greenhouse gas feedbacks, appears—based on the palaeo record—to be small under the modest warming of RCP2.6. From this perspective, staying in a range of warming experienced during the past interglacial periods is appropriate to limit risks and impacts of climate change[101]. Although these findings support the 2 °C global warming target of the Paris Agreement, more rapid or extensive warming in scenarios such as RCP8.5 would be outside the experience provided by past interglacial periods reviewed here. Such a pathway into conditions without well-studied precedent would be inherently risky for human society and sustainable development.

However, even a warming of 1.5–2 °C is sufficient to trigger substantial long-term melting of ice in Greenland and Antarctica

and cause sea-level rise that may last for millennia. For instance, the LIG and MIS11.3 were characterized by prolonged warmer-than-present-day conditions in high latitudes, leading to melting of parts of Greenland and Antarctica. This ice-sheet melt contributed to a more than 6 m sea-level rise compared to pre-industrial[16], on timescales of millennia, and caused significantly higher rates of sea-level rise compared to those of the last decades.

Comparison of palaeo data and model estimates of long-term (multi-centennial-to-millennial) warming in response to CO_2 (see Box 2) suggests that models may underestimate observed polar amplification and global mean temperatures of past warm climate states by up to a factor of two on millennial timescales. Despite the significant uncertainties in climate and CO_2 reconstructions for many of the past warm intervals, this underestimation is probably because the models lack or potentially simplify key processes such as interactive ice sheets, cloud processes and biogeochemical feedbacks that impact long-term ESS. Again, this implies that long-term sea-level rise and regional and global warming may in the long run be significantly more severe than state-of-the-art climate models project.

Knowledge gaps remain for all periods and all processes, including the reconstructions of past CO_2 concentration, air and ocean temperatures and ecosystem responses, but also for extreme events, and changes in variability (see Supplementary Information). It will be important to increase our understanding of cloud and aerosol physics, to improve the representation of cryosphere climate and biogeochemical Earth System feedbacks in climate models used for long-term projections, and to refine palaeo reconstructions as a key constraint for modelled climate sensitivity. In spite of existing uncertainties, our review of observed palaeo data and models associated with known warmer climates of the past underscores the importance of limiting the rate and extent of warming to that of past interglacial warm intervals to reduce impacts such as food and ecosystem disruptions, loss of ice, and the inundation of vast coastal areas where much of the world's population and infrastructure resides.

Data availability. All data and model results used in this Review Article are from published literature (see references provided in the main text and the Supplementary Tables).

Received: 1 December 2017; Accepted: 30 April 2018;
Published online: 25 June 2018

References

1. Morice, C. P., Kennedy, J. J., Rayner, N. A. & Jones, P. D. Quantifying uncertainties in global and regional temperature change using an ensemble of observational estimates: the HadCRUT4 data set. *J. Geophys. Res.* **117**, D08101 (2012).
2. IPCC *Climate Change 2013: The Physical Science Basis* (eds Stocker, T. F. et al.) (Cambridge Univ. Press, Cambridge, 2013).
3. Clark, P. U. et al. Consequences of twenty-first-century policy for multi-millennial climate and sea-level change. *Nat. Clim. Change* **6**, 360–369 (2016).
4. Eby, M. et al. Lifetime of anthropogenic climate change: millennial time scales of potential CO_2 and surface temperature perturbations. *J. Clim.* **22**, 2501–2511 (2009).
5. Subsidiary Body for Scientific and Technological Advice. *Report on the Structured Expert Dialogue on the 2013–2015 Review* (UNFCC, 2015).
6. Rockström, J. et al. A safe operating space for humanity. *Nature* **461**, 472 (2009).
7. Valdes, P. Built for stability. *Nat. Geosci.* **4**, 414–416 (2011).
8. Tzedakis, P. C. et al. Interglacial diversity. *Nat. Geosci.* **2**, 751–755 (2009).
9. Martinez-Boti, M. A. et al. Plio-Pleistocene climate sensitivity evaluated using high-resolution CO_2 records. *Nature* **518**, 49–54 (2015).
10. Lunt, D. J. et al. A model–data comparison for a multi-model ensemble of early Eocene atmosphere–ocean simulations: EoMIP. *Clim. Past* **8**, 1717–1736 (2012).
11. Paleosens Project Members. Making sense of palaeoclimate sensitivity. *Nature* **491**, 683–691 (2012).
12. Bentley, M. J. et al. A community-based geological reconstruction of Antarctic Ice Sheet deglaciation since the Last Glacial Maximum. *Quat. Sci. Rev.* **100**, 1–9 (2014).
13. Solomina, O. N. et al. Holocene glacier fluctuations. *Quat. Sci. Rev.* **111**, 9–34 (2015).
14. Lambeck, K., Rouby, H., Purcell, A., Sun, Y. & Sambridge, M. Sea level and global ice volumes from the Last Glacial Maximum to the Holocene. *Proc. Natl Acad. Sci. USA* **111**, 15296–15303 (2014).
15. Briner, J. P. et al. Holocene climate change in Arctic Canada and Greenland. *Quat. Sci. Rev.* **147**, 340–364 (2016).
16. Dutton, A. et al. Sea-level rise due to polar ice-sheet mass loss during past warm periods. *Science* **349**, aaa4019 (2015).
17. Colville, E. J. et al. Sr-Nd-Pb isotope evidence for ice-sheet presence on Southern Greenland during the last interglacial. *Science* **333**, 620–623 (2011).
18. DeConto, R. M. & Pollard, D. Contribution of Antarctica to past and future sea-level rise. *Nature* **531**, 591–597 (2016).
19. Sutter, J., Gierz, P., Grosfeld, K., Thoma, M. & Lohmann, G. Ocean temperature thresholds for Last Interglacial West Antarctic Ice Sheet collapse. *Geophys. Res. Lett.* **43**, 2675–2682 (2016).
20. Reyes, A. V. et al. South Greenland ice-sheet collapse during Marine Isotope Stage 11. *Nature* **510**, 525–528 (2014).
21. Schaefer, J. M. et al. Greenland was nearly ice-free for extended periods during the Pleistocene. *Nature* **540**, 252–255 (2016).
22. de Boer, B. et al. Simulating the Antarctic ice sheet in the late-Pliocene warm period: PLISMIP-ANT, an ice-sheet model intercomparison project. *Cryosphere* **9**, 881–903 (2015).
23. Dowsett, H. et al. The PRISM4 (mid-Piacenzian) paleoenvironmental reconstruction. *Clim. Past* **12**, 1519–1538 (2016).
24. Naish, T. et al. Obliquity-paced Pliocene West Antarctic ice sheet oscillations. *Nature* **458**, 322–328 (2009).
25. Cook, C. P. et al. Dynamic behaviour of the East Antarctic ice sheet during Pliocene warmth. *Nat. Geosci.* **6**, 765–769 (2013).
26. de Vernal, A., Gersonde, R., Goosse, H., Seidenkrantz, M.-S. & Wolff, E. W. Sea ice in the paleoclimate system: the challenge of reconstructing sea ice from proxies – an introduction. *Quat. Sci. Rev.* **79**, 1–8 (2013).
27. Knies, J., Cabedo-Sanz, P., Belt, S. T., Baranwal, S., Fietz, S. & Rosell-Mele, A. The emergence of modern sea ice cover in the Arctic Ocean. *Nat. Commun.* **5**, 5608 (2014).
28. Stein, R., Fahl, K., Gierz, P., Niessen, F. & Lohmann, G. Arctic Ocean sea ice cover during the penultimate glacial and the last interglacial. *Nat. Commun.* **8**, 373 (2017).
29. Spolaor, A. et al. Canadian Arctic sea ice reconstructed from bromine in the Greenland NEEM ice core. *Sci. Rep.* **6**, 33925 (2016).
30. Holloway, M. D. et al. The spatial structure of the 128 ka Antarctic sea ice minimum. *Geophys. Res. Lett.* **44**, 11129–11139 (2017).
31. Clotten, C., Stein, R., Fahl, K. & De Schepper, S. Seasonal sea ice cover during the warm Pliocene: evidence from the Iceland Sea (ODP Site 907). *Earth Planet. Sci. Lett.* **481**, 61–72 (2018).
32. Hessler, I. et al. Implication of methodological uncertainties for mid-Holocene sea surface temperature reconstructions. *Clim. Past* **10**, 2237–2252 (2014).
33. Praetorius, S. K. et al. North Pacific deglacial hypoxic events linked to abrupt ocean warming. *Nature* **527**, 362–366 (2015).
34. Duncan, B. et al. Interglacial/glacial changes in coccolith-rich deposition in the SW Pacific Ocean: an analogue for a warmer world? *Glob. Planet. Chang.* **144**, 252–262 (2016).
35. Studer, A. S. et al. Antarctic zone nutrient conditions during the last two glacial cycles. *Paleoceanography* **30**, 845–862 (2015).
36. Jaccard, S. L. et al. Two modes of change in Southern Ocean productivity over the past million years. *Science* **339**, 1419–1423 (2013).
37. Sigman, D. M., Jaccard, S. L. & Haug, G. H. Polar ocean stratification in a cold climate. *Nature* **428**, 59–63 (2004).
38. Cane, T., Rohling, E. J., Kemp, A. E. S., Cooke, S. & Pearce, R. B. High-resolution stratigraphic framework for Mediterranean sapropel S5: defining temporal relationships between records of Eemian climate variability. *Palaeogeogr. Palaeoclimatol. Palaeoecol.* **183**, 87–101 (2002).
39. Kender, S. et al. Mid Pleistocene foraminiferal mass extinction coupled with phytoplankton evolution. *Nat. Commun.* **7**, 11970 (2016).
40. Haywood, A. M., Dowsett, H. J. & Dolan, A. M. Integrating geological archives and climate models for the mid-Pliocene warm period. *Nat. Commun.* **7**, 10646 (2016).
41. Yasuhara, M., Hunt, G., Breitburg, D., Tsujimoto, A. & Katsuki, K. Human-induced marine ecological degradation: micropaleontological perspectives. *Ecol. Evol.* **2**, 3242–3268 (2012).
42. Jolly, D., Harrison, S. P., Damnati, B. & Bonnefille, R. Simulated climate and biomes of Africa during the Late Quarternary: comparison with pollen and lake status data. *Quat. Sci. Rev.* **17**, 629–657 (1998).
43. Williams, J. W., Shuman, B. & Bartlein, P. J. Rapid responses of the prairie-forest ecotone to early Holocene aridity in mid-continental North America. *Glob. Planet. Chang.* **66**, 195–207 (2009).

44. Reasoner, M. & Tinner, W. in *Encyclopedia of Paleoclimatology and Ancient Environments* (ed. Gornitz, V.) 442–446 (Springer, Dordrecht, 2008).
45. Bigelow, N. H. Climate change and Arctic ecosystems: 1. vegetation changes north of 55°N between the last glacial maximum, mid-Holocene, and present. *J. Geophys. Res.* **108**, 8170 (2003).
46. CAPE-Last Interglacial Project Members. Last Interglacial Arctic warmth confirms polar amplification of climate change. *Quat. Sci. Rev.* **25**, 1383–1400 (2006).
47. Larrasoaña, J. C., Roberts, A. P. & Rohling, E. J. Dynamics of Green Sahara periods and their role in hominin evolution. *PLoS ONE* **8**, e76514 (2013).
48. de Vernal, A. & Hillaire-Marcel, C. Natural variability of Greenland climate, vegetation, and ice volume during the past million years. *Science* **320**, 1622–1625 (2008).
49. Helmens, K. F. et al. Major cooling intersecting peak Eemian Interglacial warmth in northern Europe. *Quat. Sci. Rev.* **122**, 293–299 (2015).
50. Melles, M. et al. 2.8 million years of Arctic climate change from Lake El'gygytgyn, NE Russia. *Science* **337**, 315–320 (2012).
51. Urrego, D. H., Sánchez Goñi, M. F., Daniau, A. L., Lechevrel, S. & Hanquiez, V. Increased aridity in southwestern Africa during the warmest periods of the last interglacial. *Clim. Past* **11**, 1417–1431 (2015).
52. Andreev, A. A. et al. Late Pliocene and Early Pleistocene vegetation history of northeastern Russian Arctic inferred from the Lake El'gygytgyn pollen record. *Clim. Past* **10**, 1017–1039 (2014).
53. Lemoine, D. & Traeger, C. P. Economics of tipping the climate dominoes. *Nat. Clim. Change* **6**, 514–519 (2016).
54. Schilt, A. et al. Isotopic constraints on marine and terrestrial N_2O emissions during the last deglaciation. *Nature* **516**, 234–237 (2014).
55. Marcott, S. A. et al. Centennial-scale changes in the global carbon cycle during the last deglaciation. *Nature* **514**, 616–619 (2014).
56. Rhodes, R. H. et al. Enhanced tropical methane production in response to iceberg discharge in the North Atlantic. *Science* **348**, 1016 (2015).
57. Frank, D. C. et al. Ensemble reconstruction constraints on the global carbon cycle sensitivity to climate. *Nature* **463**, 527–530 (2010).
58. Bauska, T. K. et al. Links between atmospheric carbon dioxide, the land carbon reservoir and climate over the past millennium. *Nat. Geosci.* **8**, 383–387 (2015).
59. Charman, D. J. et al. Climate-related changes in peatland carbon accumulation during the last millennium. *Biogeosciences* **10**, 929–944 (2013).
60. Frolking, S. & Roulet, N. T. Holocene radiative forcing impact of northern peatland carbon accumulation and methane emissions. *Glob. Change Biol.* **13**, 1079–1088 (2007).
61. Stocker, B. D., Yu, Z., Massa, C. & Joos, F. Holocene peatland and ice-core data constraints on the timing and magnitude of CO_2 emissions from past land use. *Proc. Natl Acad. Sci. USA* **114**, 1492–1497 (2017).
62. Yu, Z., Loisel, J., Brosseau, D. P., Beilman, D. W. & Hunt, S. J. Global peatland dynamics since the Last Glacial Maximum. *Geophys. Res. Lett.* **37**, (2010).
63. Dalton, A. S., Finkelstein, S. A., Barnett, P. J. & Forman, S. L. Constraining the Late Pleistocene history of the Laurentide Ice Sheet by dating the Missinaibi Formation, Hudson Bay Lowlands, Canada. *Quat. Sci. Rev.* **146**, 288–299 (2016).
64. Sierralta, M., Urban, B., Linke, G. & Frechen, M. Middle Pleistocene interglacial peat deposits from Northern Germany investigated by 230Th/U and palynology: case studies from Wedel and Schöningen. *Zeitschrift der Deutschen Gesellschaft für Geowissenschaften* **168**, 373–387 (2017).
65. Mitchell, W. T. et al. Stratigraphic and paleoenvironmental reconstruction of a mid-Pliocene fossil site in the High Arctic (Ellesmere Island, Nunavut): evidence of an ancient peatland with beaver activity. *Arctic* **69**, 185–204 (2016).
66. Turetsky, M. R. et al. Global vulnerability of peatlands to fire and carbon loss. *Nat. Geosci.* **8**, 11–14 (2015).
67. Hugelius, G. et al. Estimated stocks of circumpolar permafrost carbon with quantified uncertainty ranges and identified data gaps. *Biogeosciences* **11**, 6573–6593 (2014).
68. Bock, M. et al. Glacial/interglacial wetland, biomass burning and geologic methane emissions constrained by dual stable isotopic CH_4 ice core records. *Proc. Natl Acad. Sci. USA* **114**, 5778–5786 (2017).
69. Bereiter, B. et al. Revision of the EPICA Dome C CO_2 record from 800 to 600 kyr before present. *Geophys. Res. Lett.* https://doi.org/10.1002/2014GL061957 (2015).
70. Loulergue, L. et al. Orbital and millennial-scale features of atmospheric CH_4 over the past 800,000 years. *Nature* **453**, 383–386 (2008).
71. Köhler, P., Knorr, G. & Bard, E. Permafrost thawing as a possible source of abrupt carbon release at the onset of the Bølling/Allerød. *Nat. Commun.* **5**, 5520 (2014).
72. Kennett, J. P., Cannariato, K. G., Hendy, I. L. & Behl, R. J. Carbon isotopic evidence for methane hydrate instability during Quaternary interstadials. *Science* **288**, 128–133 (2000).
73. Bock, M. et al. Hydrogen isotopes preclude clathrate CH_4 emissions at the onset of Dansgaard-Oeschger events. *Science* **328**, 1686–1689 (2010).
74. Petrenko, V. V. et al. Minimal geological methane emissions during the Younger Dryas–Preboreal abrupt warming event. *Nature* **548**, 443–446 (2017).
75. MacDougall, A. H. & Knutti, R. Projecting the release of carbon from permafrost soils using a perturbed parameter ensemble modelling approach. *Biogeosciences* **13**, 2123–2136 (2016).
76. Gregory, J. M. & Huybrechts, P. Ice-sheet contributions to future sea-level change. *Philos. Trans. R. Soc. Lond. A* **354**, 1709–1731 (2006).
77. Robinson, A., Calov, R. & Ganopolski, A. Multistability and critical thresholds of the Greenland ice sheet. *Nat. Clim. Change* **2**, 429–432 (2012).
78. Hatfield, R. G. et al. Interglacial responses of the southern Greenland ice sheet over the last 430,000 years determined using particle-size specific magnetic and isotopic tracers. *Earth Planet. Sci. Lett.* **454**, 225–236 (2016).
79. Yau, A. M., Bender, M. L., Blunier, T. & Jouzel, J. Setting a chronology for the basal ice at Dye-3 and GRIP: implications for the long-term stability of the Greenland Ice Sheet. *Earth Planet. Sci. Lett.* **451**, 1–9 (2016).
80. Bierman, P. R., Shakun, J. D., Corbett, L. B., Zimmerman, S. R. & Rood, D. H. A persistent and dynamic East Greenland Ice Sheet over the past 7.5 million years. *Nature* **540**, 256–260 (2016).
81. Scherer, R. P., Aldahan, A., Tulaczyk, S., Possnert, G., Engelhardt, H. & Kamb, B. Pleistocene collapse of the West Antarctic ice sheet. *Science* **281**, 82–85 (1998).
82. Barnes, D. K. A. & Hillenbrand, C.-D. Faunal evidence for a late quaternary trans-Antarctic seaway. *Glob. Change Biol.* **16**, 3297–3303 (2010).
83. Williams, T. et al. Evidence for iceberg armadas from East Antarctica in the Southern Ocean during the late Miocene and early Pliocene. *Earth Planet. Sci. Lett.* **290**, 351–361 (2010).
84. Golledge, N. R., Levy, R. H., McKay, R. M. & Naish, T. R. East Antarctic ice sheet most vulnerable to Weddell Sea warming. *Geophys. Res. Lett.* **44**, 2343–2351 (2017).
85. Steig, E. J. et al. Influence of West Antarctic ice sheet collapse on Antarctic surface climate. *Geophys. Res. Lett.* **42**, 4862–4868 (2015).
86. Vaughan, D. G., Barnes, D. K. A., Fretwell, P. T. & Bingham, R. G. Potential seaways across West Antarctica. *Geochem. Geophys.* **12**, Q10004 (2011).
87. Hay, C. C., Morrow, E., Kopp, R. E. & Mitrovica, J. X. Probabilistic reanalysis of twentieth-century sea-level rise. *Nature* **517**, 481–484 (2015).
88. Kopp, R. E., Simons, F. J., Mitrovica, J. X., Maloof, A. C. & Oppenheimer, M. A probabilistic assessment of sea level variations within the last interglacial stage. *Geophys. J. Int.* **193**, 711–716 (2013).
89. O'Leary, M. J. et al. Ice sheet collapse following a prolonged period of stable sea level during the last interglacial. *Nat. Geosci.* **6**, 796–800 (2013).
90. Rohling, E. J. et al. High rates of sea-level rise during the last interglacial period. *Nat. Geosci.* **1**, 38–42 (2007).
91. Nerem, R. S. et al. Climate-change-driven accelerated sea-level rise detected in the altimeter era. *Proc. Natl Acad. Sci. USA* **115**, 2022–2025 (2018).
92. Tinner, W. et al. A 700-year paleoecological record of boreal ecosystem responses to climatic variation from Alaska. *Ecology* **89**, 729–743 (2008).
93. Schwörer, C., Henne, P. D. & Tinner, W. A model-data comparison of Holocene timberline changes in the Swiss Alps reveals past and future drivers of mountain forest dynamics. *Glob. Change Biol.* **20**, 1512–1526 (2014).
94. Verbesselt, J. et al. Remotely sensed resilience of tropical forests. *Nat. Clim. Change* **6**, 1028–1031 (2016).
95. MacDonald, G. M., Kremenetski, K. V. & Beilman, D. W. Climate change and the northern Russian treeline zone. *Philos. Trans. R. Soc. Lond. B Biol. Sci.* **363**, 2285–2299 (2008).
96. Scheffer, M., Hirota, M., Holmgren, M., Van Nes, E. H. & Chapin, F. S. Thresholds for boreal biome transitions. *Proc. Natl Acad. Sci. USA* **109**, 21384–21389 (2012).
97. Ruosch, M., Spahni, R., Joos, F., Henne, P. D., van der Knaap, W. O. & Tinner, W. Past and future evolution of Abies alba forests in Europe - comparison of a dynamic vegetation model with palaeo data and observations. *Glob. Change Biol.* **22**, 727–740 (2016).
98. Colombaroli, D. et al. Response of broadleaved evergreen Mediterranean forest vegetation to fire disturbance during the Holocene: insights from the peri-Adriatic region. *J. Biogeogr.* **36**, 314–326 (2009).
99. Hirota, M., Holmgren, M., Van Nes, E. H. & Scheffer, M. Global resilience of tropical forest and savanna to critical transitions. *Science* **334**, 232–235 (2011).
100. Kröpelin, S. et al. Climate-driven ecosystem succession in the Sahara: the past 6000 years. *Science* **320**, 765–768 (2008).
101. *The Paris Agreement* (UN Treaty Collection, 2015).
102. Ceballos, G., Ehrlich, P. R. & Dirzo, R. Biological annihilation via the ongoing sixth mass extinction signaled by vertebrate population losses and declines. *Proc. Natl Acad. Sci. USA* **114**, E6089–E6096 (2017).

103. Snyder, C. W. Evolution of global temperature over the past two million years. *Nature* **538**, 226–228 (2016).
104. Hansen, J., Sato, M., Russell, G. & Kharecha, P. Climate sensitivity, sea level and atmospheric carbon dioxide. *Philos. Trans. A Math. Phys. Eng. Sci.* **371**, 20120294 (2013).
105. Bartoli, G., Hönisch, B. & Zeebe, R. E. Atmospheric CO_2 decline during the Pliocene intensification of Northern Hemisphere glaciations. *Paleoceanography* **26**, PA4213 (2011).
106. Hönisch, B., Hemming, N. G., Archer, D., Siddall, M. & McManus, J. Atmospheric carbon dioxide concentration across the Mid-Pleistocene transition. *Science* **324**, 1551–1554 (2009).
107. Marcott, S. A., Shakun, J. D., Clark, P. U. & Mix, A. C. A reconstruction of regional and global temperature for the past 11,300 years. *Science* **339**, 1198–1201 (2013).
108. PAGES2k Consortium. A global multiproxy database for temperature reconstructions of the Common Era. *Sci. Rep.* **4**, 170088 (2017).
109. Hoffman, J. S., Clark, P. U., Parnell, A. C. & He, F. Regional and global sea-surface temperatures during the last interglaciation. *Science* **355**, 276–279 (2017).
110. Otto-Bliesner, B. L. et al. How warm was the last interglacial? New model–data comparisons. *Philos. Trans. A Math Phys. Eng. Sci.* **371**, 20130097 (2013).
111. Barber, D. C. et al. Forcing of the cold event of 8,200 years ago by catastrophic drainage of Laurentide lakes. *Nature* **400**, 344–348 (1999).
112. Schilt, A. et al. Atmospheric nitrous oxide during the last 140,000 years. *Earth Planet. Sci. Lett.* **300**, 33–43 (2010).
113. Berger, A. & Loutre, M. F. Insolation values for the climate of the last 10 million years. *Quat. Sci. Rev.* **10**, 297–317 (1991).
114. Marsicek, J., Shuman, B. N., Bartlein, P. J., Shafer, S. L. & Brewer, S. Reconciling divergent trends and millennial variations in Holocene temperatures. *Nature* **554**, 92–96 (2018).
115. Kobashi, T. et al. Volcanic influence on centennial to millennial Holocene Greenland temperature change. *Sci. Rep.* **7**, 1441 (2017).
116. Vinther, B. et al. Holocene thinning of the Greenland ice sheet. *Nature* **461**, 385–388 (2009).
117. Buizert, C. et al. Greenland-wide seasonal temperatures during the last deglaciation. *Geophys. Res. Lett.* **45**, 1905–1914 (2018).
118. Eldevik, T. et al. A brief history of climate – the northern seas from the Last Glacial Maximum to global warming. *Quat. Sci. Rev.* **106**, 225–246 (2014).
119. Max, L. et al. Sea surface temperature variability and sea-ice extent in the subarctic northwest Pacific during the past 15,000 years. *Paleoceanography* **27**, PA3213 (2012).
120. Barron, J. A., Heusser, L., Herbert, T. & Lyle, M. High-resolution climatic evolution of coastal northern California during the past 16,000 years. *Paleoceanography* **18**, 1020 (2003).
121. Clark, P. U. & Huybers, P. Interglacial and future sea level. *Nature* **462**, 856–857 (2009).
122. McKay, N. P., Overpeck, J. T. & Otto-Bliesner, B. L. The role of ocean thermal expansion in Last Interglacial sea level rise. *Geophys. Res. Lett.* **38**, L14605 (2011).
123. CLIMAP Project Members. The last interglacial ocean. *Quat. Res.* **21**, 123–224 (1984).
124. Turney, C. S. M. & Jones, R. T. Does the Agulhas Current amplify global temperatures during super-interglacials? *J. Quat. Sci.* **25**, 839–843 (2010).
125. Capron, E., Govin, A., Feng, R., Otto-Bliesner, B. L. & Wolff, E. W. Critical evaluation of climate syntheses to benchmark CMIP6/PMIP4 127 ka last interglacial simulations in the high-latitude regions. *Quat. Sci. Rev.* **168**, 137–150 (2017).
126. Landais, A. et al. How warm was Greenland during the last interglacial period? *Clim. Past* **12**, 1933–1948 (2016).
127. Dowsett, H. J. et al. Assessing confidence in Pliocene sea surface temperatures to evaluate predictive models. *Nat. Clim. Change* **2**, 365–371 (2012).
128. Brigham-Grette, J. et al. Pliocene warmth, polar amplification, and stepped pleistocene cooling recorded in NE Arctic Russia. *Science* **340**, 1421–1427 (2013).
129. Ballantyne, A. P., Greenwood, D. R., Sinninghe Damsté, J. S., Csank, A. Z., Eberle, J. J. & Rybczynski, N. Significantly warmer Arctic surface temperatures during the Pliocene indicated by multiple independent proxies. *Geology* **38**, 603–606 (2010).
130. Salzmann, U. et al. Challenges in quantifying Pliocene terrestrial warming revealed by data–model discord. *Nat. Clim. Change* **3**, 969–974 (2013).
131. Lea, D. W. The 100 000-yr cycle in tropical SST, greenhouse forcing, and climate sensitivity. *J. Clim.* **17**, 2170–2179 (2004).
132. Dyez, K. A. & Ravelo, A. C. Late Pleistocene tropical Pacific temperature sensitivity to radiative greenhouse gas forcing. *Geology* **41**, 23–26 (2013).
133. Lunt, D. J., Haywood, A. M., Schmidt, G. A., Salzmann, U., Valdes, P. J. & Dowsett, H. J. Earth system sensitivity inferred from Pliocene modelling and data. *Nat. Geosci.* **3**, 60–64 (2010).
134. von der Heydt, A. S. et al. Lessons on climate sensitivity from past climate changes. *Curr. Clim. Change Rep.* **2**, 148–158 (2016).
135. Meissner, K. J. et al. The Paleocene-Eocene Thermal Maximum: how much carbon is enough? *Paleoceanography* **29**, 946–963 (2014).
136. Anagnostou, E. et al. Changing atmospheric CO_2 concentration was the primary driver of early Cenozoic climate. *Nature* **533**, 380–384 (2016).
137. Goldner, A., Huber, M. & Caballero, R. Does Antarctic glaciation cool the world? *Clim. Past* **9**, 173–189 (2013).
138. Kiehl, J. T. & Shields, C. A. Sensitivity of the Palaeocene–Eocene Thermal Maximum climate to cloud properties. *Phil. Trans. R. Soc. A* **371**, 20130093 (2013).
139. Sagoo, N., Valdes, P., Flecker, R. & Gregoire, L. J. The Early Eocene equable climate problem: can perturbations of climate model parameters identify possible solutions? *Phil. Trans. R. Soc. A* **371**, 20130123 (2013).

Acknowledgements

Financial support of the PAGES Warmer World Integrative Activity workshop by the Future Earth core project PAGES (Past Global Changes) and the Oeschger Centre for Climate Change Research, University of Bern, is gratefully acknowledged. Additional funding by PAGES was provided to the plioVAR, PALSEA 2, QUIGS, the 2k network, C-peat, Global Paleofire 2 and OC3 PAGES working groups contributing to the Integrated Activity (see http://www.pages.unibe.ch/science/intro for an overview of all former and active PAGES working groups). We thank N. Rosenbloom for creating Fig. 2.

Author contributions

The content of this paper is the result of a PAGES workshop taking place in Bern, Switzerland, in April 2017, which most of the authors attended. All authors contributed to the literature assessment and the discussion of the results. H.F., K.J.M. and A.C.M. developed the concept of the paper and compiled the paper with support by all co-authors. All co-authors contributed to the discussion of the manuscript.

Competing interests

The authors declare no competing interests.

Additional information

Supplementary information is available for this paper at https://doi.org/10.1038/s41561-018-0146-0.

Reprints and permissions information is available at www.nature.com/reprints.

Correspondence should be addressed to H.F. or K.J.M. or A.C.M.

[1]Climate and Environmental Physics, Physics Institute, University of Bern, Bern, Switzerland. [2]Oeschger Centre for Climate Change Research, University of Bern, Bern, Switzerland. [3]Climate Change Research Centre, University of New South Wales Sydney, ARC Centre of Excellence for Climate System Science, Sydney, Australia. [4]College of Earth, Ocean, and Atmospheric Sciences, Oregon State University, Corvallis, OR, USA. [5]Research School of Earth Sciences, The Australian National University, ARC Centre of Excellence for Climate Extremes, Canberra, Australia. [6]Bullard Laboratories, Department of Earth Sciences, University of Cambridge, Cambridge, UK. [7]Max Planck Institute for Meteorology, Hamburg, Germany. [8]Centre for Ice and Climate, Niels Bohr Institute, University of Copenhagen, Copenhagen, Denmark. [9]British Antarctic Survey, Cambridge, UK. [10]Centre for Quaternary Research, Department of Geography, Royal Holloway University of London, Egham, Surrey, UK. [11]Institute of Plant Sciences, University of Bern, Bern, Switzerland. [12]Limnology Unit, Department of Biology, Ghent University, Ghent, Belgium. [13]Environnements et Paléoenvironnements Océaniques et Continentaux, EPOC, CNRS, Université de Bordeaux, Pessac, France. [14]Lamont-Doherty Earth Observatory, Columbia University, Palisades, NY, USA. [15]MARUM - Center for Marine Environmental Sciences, University of Bremen, Bremen, Germany. [16]Department of Earth Sciences, University of Toronto, Toronto, Canada. [17]Institute of Geological Sciences, University of Bern, Bern, Switzerland. [18]Department of Geography, Durham University, Durham, United Kingdom. [19]Leibniz Center for Tropical Marine Ecology, Bremen, Germany. [20]Alfred Wegener Institute, Helmholtz Centre for Polar and Marine Research, Bremerhaven, Germany. [21]Department of Earth Sciences, University of Cambridge, Cambridge, UK. [22]International Foundation High Altitude Research Stations Jungfraujoch and Gornergrat, Bern, Switzerland. [23]Institute for Environmental Sciences and Dendrolab, Department of Earth Sciences, University of Geneva, Geneva, Switzerland. [24]Institute for the Dynamics of Environmental Processes - CNR, Venice, Italy. [25]Department of Environmental Sciences, Informatics and Statistics, Ca'Foscari University of Venice, Venice, Italy. [26]Institute of Ecology and Geography, Siberian Federal University, Krasnoyarsk, Russia. [27]GNS Science, Lower Hutt, New Zealand. [28]Department of Biology, Queen's University, Kingston, Canada. [29]Institute of Earth Surface Dynamics, University of Lausanne, Lausanne, Switzerland. [30]Centre de recherche en géochimie et géodynamique, Université du Québec à Montréal, Montréal, Canada. [31]Department of Earth Sciences, University of Southern California, Los Angeles, CA, USA. [32]Department of Earth and Atmospheric Sciences, University of Nebraska-Lincoln, Lincoln, NE, USA. [33]Past Global Changes (PAGES), Bern, Switzerland. [34]School of Geographical Sciences and Cabot Institute, University of Bristol, Bristol, UK. [35]Laboratory of Wetland Ecology and Monitoring, Department of Biogeography and Palaeoecology, Faculty of Geographical and Geological Sciences, Adam Mickiewicz University, Poznań, Poland. [36]School of Forestry and Environmental Studies, Yale University, New Haven, CT, USA. [37]Laboratoire des Sciences du Climat et de l'Environnement, Institut Pierre Simon Laplace (UMR8212 CEA-CNRS-UVSQ, Université Paris Saclay), Gif-sur-Yvette cédex, France. [38]Climate and Global Dynamics Laboratory, National Center for Atmospheric Research, Boulder, CO, USA. [39]Uni Research Climate, Bjerknes Centre for Climate Research, Bergen, Norway. [40]École Pratique des Hautes Études, EPHE, PSL University, Paris, France. [41]United States Global Change Research Program, National Coordination Office, Washington, DC, USA. [42]Institute for Geosciences, University of Kiel, Kiel, Germany. [43]Quaternary Sciences, Department of Geology, Lund University, Lund, Sweden. [44]Nansen-Zhu International Research Centre, Institute of Atmospheric Physics, Chinese Academy of Sciences, Beijing, China. [45]Department of Earth and Environmental Sciences, Lehigh University, Bethlehem, PA, USA. [46]Institute for Peat and Mire Research, School of Geographical Sciences, Northeast Normal University, Changchun, China. [47]Department of Earth Sciences, Faculty of Geosciences, Utrecht University, Utrecht, The Netherlands. [48]Geological Institute, ETH Zürich, Zürich, Switzerland. [49]Laboratory for Earth Surface Processes, Department of Geography, Institute of Ocean Research, Peking University, Beijing, China. *e-mail: hubertus.fischer@climate.unibe.ch; k.meissner@unsw.edu.au; mix@coas.oregonstate.edu